BCL-13: A 13-DOF Soft Robotic Hand for Dexterous Grasping and In-hand Manipulation

Jianshu Zhou, *Student Member*, *IEEE*, Juan Yi, *Student Member*, *IEEE*, Xiaojiao Chen, *Student Member*, *IEEE*, Zixie Liu and Zheng Wang* *Senior Member*, *IEEE*

Abstract*—This paper presents a dexterous soft robotic hand, BCL-13, with 4 fingers and 13 independently-actuated joints capable of in-hand manipulation. The iconic dexterity is enabled by a novel soft robotic finger design with 3 DOFs, significantly improving over existing soft actuator dexterity and realizing human-finger-like workspace. The palm is also equipped with a dedicated rotational DOF to enable opposition of fingers. Investigations on human hand model reduction, in-hand manipulation principles, as well as the fabrication procedures of the soft robotic fingers and hand were presented in detail. Dedicated experiments using the fabricated prototypes were conducted to evaluate the effectiveness of proposed robotic anthropomorphic system via a series of workspace, grasping, and in-hand manipulation tasks. The proposed BCL-13 hand offers a promising design solution to a light weight, dexterous, affordable, and highly anthropomorphic robotic hand design.

I. INTRODUCTION

Human hand dexterity is amongst our most distinguished features, enabling abundant grasping taxonomies to various objects, and even in-hand manipulation of small objects [1], they have been the top design objectives for robotic hands [2-4]. Conventional multi-fingered robotic hands and prosthetics have rigid structures, achieving dexterous grasping and in-hand manipulation [5-9]. Under-actuation and cable-transmission have been utilized by various designs to improve safety and adaptability limited by rigid mechanisms [10-13]. Although pioneering robotic hands with a high degree-of-freedom (DOF) numbers have achieved close-to-human hand dexterity, their heavy reliance on mechanism complexity also gave rise to various challenges from complexity, serviceability, transmission loss, to behavior sensing, control, and cost [5-14].

Addressing the challenges of rigid robotic hands, nature provides abundant examples of passive compliance [15], as inspirations for robotic hand designs [16]. Primarily composed of intrinsically soft materials, the inherent compliance of soft robotic hands could adapt to object shapes without proactive control, and absorbs energy during impact,

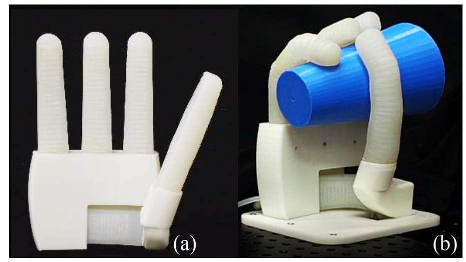

Figure.1. (a) The BCL-13 soft robotic hand with 13 independent DOF. (b) BCL-13 successfully grasps a 3D-printed frustum.

with excellent interaction safety. Soft robotic hands are often with lower requirements on structural, sensing, and actuation elements than rigid ones. Following global research efforts in recent years, various soft robotic hands have been reported for adaptable and reliable grasping of delicate objects, from the early-age soft-robotic grippers with two or three digits with target conformability [17-21], to anthropomorphism designs of multi-digit soft robotic hands achieving human-like grasping taxonomies [22], as well as detecting physical interactions [23]. However, limited by soft robotic design and fabrication techniques, state-of-the-art soft robotic hands are with 3-5 DOF and limited with single-DOF fingers, significantly lower than rigid hands [15, 16, 24]. With the highly limited dexterity, in-hand manipulation is a major challenge for state-of-the-art soft robotic hands [15, 24, 25].

This paper tackles in-hand manipulation for soft robotic hand by proposing a 13-DOF anthropomorphic design, the BCL-13 (Figure 1), achieving excellent grasping capabilities and three in-hand manipulation modes. The distinctive dexterity is enabled by a novel 3-DOF soft robotic finger design with human-like planer reachable area, substantially expanded from the single-curve motion trajectory of the 1-DOF soft fingers. Experiments are conducted on the BCL-13 to validate grasping and in-hand manipulation capabilities.

II. DESIGN OF THE BCL-13 HAND

A. Human Hand Model Analysis and Reduction

Human hand is a masterpiece of nature with outstanding capabilities of grasping and manipulation. Various human hand kinematic models have been proposed for grasping analysis and robotic hand design, a commonly-accepted 23-DOF model is presented in Figure 2a [1, 4, 5, 33], with the thumb having 5 DOF and 4 DOF on each other four fingers, the last 2 DOFs are at the base of ring and little finger, respectively. Studies from various previous works on in-hand manipulation suggested that the key to in-hand manipulation lies in the common workspace between opposing fingers [2, 3, 4, 5, 9, 10]. Each finger, with flexion and extension, can be

Manuscript received: February 22, 2018; Revised: May 19, 2018; Accepted: June 18, 2018.

This paper was recommended for publication by Editor H. Ding upon evaluation of the Associate Editor and Reviewers' comments. The presented research has been supported by Hong Kong RGC-ECS Grant 27210315, HKU Funding for Basic Research 201511159051 and 201611159196.

J. Zhou, X. Chen, J. Yi, Z. Liu and Z. Wang are with the Department of Mechanical Engineering, the University of Hong Kong, Pokfulam, Hong Kong SAR, China (email: zhoujs@hku.hk, yijuan@hku.hk, chen2014@hku.hk, liuzixie@hku.hk, zwangski@hku.hk).

*Corresponding author, e-mail:zwangski@hku.hk, Tel: +852-3917-7905, Fax: +852-2858-5415.

Digital Object Identifier (DOI): see top of this page.

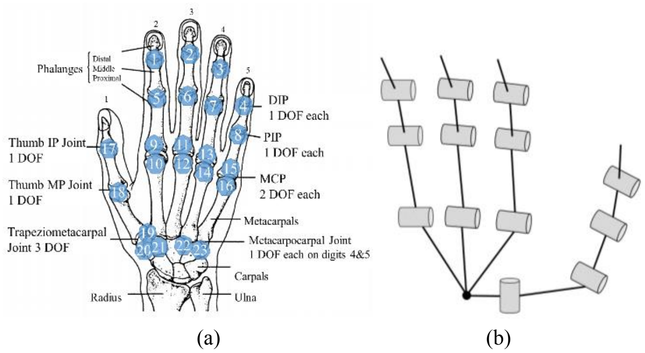

Figure.2. Human hand model reduction (a) A 23-DOF model of the human hand. (b) The simplified 13-DOF model of the proposed soft robotic hand. Each finger has 3 DOFs for MCP, DIP, and PIP joints (1-12). Palm has one bending DOF 13.

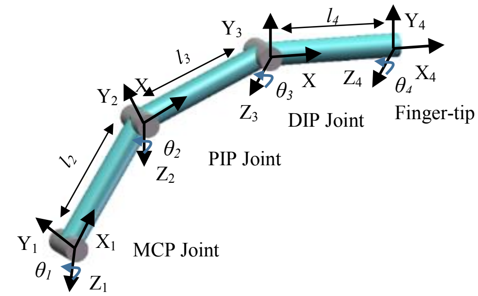

Figure.3. Kinematic sketch of three links model of human finger

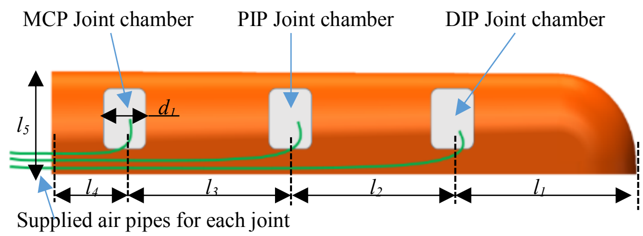

Figure.4. The structure of the fully-actuated soft robotic finger.

characterized by a 3-DOF kinematic model in Figure 3 [5].

The reachable area of the finger-tip, considering each finger joint range limits, forms a planar area with a crescent shape [26]. To facilitate in-hand manipulation, a common workspace (intersection of reachable areas) must be achieved between adjacent or opposing fingers. The larger and more complex the common workspace, the more in-hand manipulation capability [2, 3, 4, 5, 9, 10]. Therefore, the following two factors are critical for in-hand manipulation:

1) Large reachable areas for each finger,
2) Large intersections amongst fingers.

Unfortunately, neither factor could be easily achieved by existing soft robotic hands, as the commonly-adopted 1-DOF soft finger design with a continuum chamber could only achieve single-curve trajectory instead of an area.

Bridging the gap between state-of-the-art 3-5 DOF soft hands to the human dexterity, a model reduction is performed on the 23-DOF human hand model, to focus on the essential factors specifically for in-hand manipulation (Figure 2b):

1) The thumb and 3 opposing fingers are chosen to reflect the major fingers involved in in-hand manipulation tasks, as the ring and little finger motions are often coupled in manipulation tasks [1],

2) Each finger has 3 bending DOF (DOF 1-12) as they are essential to create a large finger workspace,

3) The 1-DOF palm (DOF-13) in replacement of the 4 DOFs on the human model, to create thumb rotation and form the critical common workspace between fingers.

Resulting from the model reduction, a 4-fingered 13-DOF robotic hand model is illustrated in Figure 2b. Further expansion from 4-finger to 5-finger design, if necessary, could be easily achieved in future investigations.

B. 3 Modes of In-hand Manipulation

Three modes of in-hand manipulations are demonstrated for the BCL-13 hand in this work:

Mode 1: Two fingers pinch an object and move along a path in space without contact point change.

Mode 2: Two fingers pinch an object and rotate with changing contact points.

Mode 3: Two fingers pinch an object, with its orientation adjusted by a third finger.

While the above-listed three primitive modes of in-hand manipulations can be realized by the proposed 13-DOF hand

Table I. Parameters of proposed 3-DOFs soft robotic finger

Inner chamber thickness (mm)	2	MCP length/l3(mm)	40
Outer chamber thickness (mm)	2	Finger base length/l4(mm)	15
Joint chamber length/d1 (mm)	18	Finger-tip width(mm)	18
DIP length/l1(mm)	25	Finger base width(mm)	25
PIP length/l2(mm)	30	Finger thickness(mm)	20

design, the range of each mode will be highly dependent on the designs of each finger and the overall system. In addition, more dexterous manipulations could be composed using the primitives for further functionalities.

C. Design of 3-DOF Fully-actuated Soft Robotic Finger

A novel 3-DOF soft robotic finger is proposed to realize the in-hand manipulation capability as discussed in Section II.B. Each finger is a 3-DOF soft pneumatic actuator (SPA), achieving human-finger-comparable reachability.

One of the unique characteristics of soft actuators is their mechanical programmability, such that using a simple actuation input could achieve complex pre-defined motions [16, 25, 29]. However, for each actuator the motion is largely pre-determined along the pre-defined trajectory. In order to achieve a planar reachable space, multiple actuated segments are required. Our previous work has demonstrated the substantial performance improvements of using 2-DOF soft robotic fingers for grasping tasks [19]. In this work a 3-DOF soft finger design is proposed to achieve an even larger reachable space, to facilitate in-hand manipulation.

Taking a multi-chamber approach, the proposed 3-DOF SPA design is illustrated in Figure 4, with design parameters presented in Table I. Three separated chambers are arranged for the function of DIP, PIP, and MCP joints respectively. Each chamber is actuated independently with a separated air supply tube integrated at the finger base. The phalanges are molded from soft silicone rubber materials, and the length of phalange is selected based on typical human middle finger [1]. The inner chamber has hemi-circular cross section to improve force capability for grasping [25, 27, 29].

This article has been accepted for publication in a future issue of this journal, but has not been fully edited. Content may change prior to final publication. Citation information: DOI 10.1109/LRA.2018.2851360, IEEE Robotics and Automation Letters

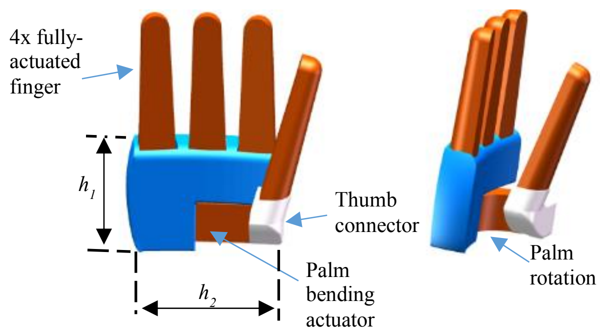

Figure 5. The 13-DOF anthropomorphic soft robotic hand design. Four 3-DOF fingers with 1-DOF palm.

D. Design of BCL-13

Following the discussion in Section II.A, a 4-fingered robotic hand is proposed as illustrated in Figure 5. The hand features one thumb and 3 opposing fingers. Each finger has 3-DOF, and the palm equips one DOF for rotating the thumb to an opposing configuration both for grasping and in-hand manipulation tasks. Taking anthropomorphism consideration, the palm resembles human palm size with height h1=80 mm and width h2=110 mm. The majority of the palm is rigid, except a soft bending actuator of length 60 mm as the palm DOF. The length of palm actuator is selected such that under its maximum deformation, the thumb could be opposing the middle finger, coinciding their reachable planes. The thumb is perpendicular to the palm actuator via a rigid connector with a 30-degree outward incline to increase the grasping volume of the proposed soft hand.

III. Fabrication and Control

A. Fabrication of BCL-13

The 3-DOF fully actuated soft robotic finger can be fabricated following the processes illustrated in Figure 6, a refined multi-chamber SPA fabrication approach from existing procedures often used in existing works [19,22,25,29]. The fabrication procedure for conventional single-chamber SPAs molds the lateral surface of chamber first and then seal the ends. We mold the head and bottom of each chamber first, then seals three chambers and leave a groove for air pipes (Figure 6a-b). By inserting the air pipes through side wall, (Figure 6.c), the air pipes can be sealed by the limiting layer and winded fiber without the need of rigid sealing components such as claps. Thus the SPA is self-sealed keeping highly flexibility and compliance.

The pipes in this design are 2 mm in diameter, and the width of the groove is 6 mm. The inner chamber is then winded with reinforced fibers, followed by casting the outer upper skin of the inner mold. Finally the bottom skin of soft finger is cast by a surface mold, towards the final soft robotic finger as shown in Figure 6.g. Dragon-skin-10 is used to fabricate all soft finger components. The palm actuator is a single chamber soft actuator with rectangular cross section. The parameters are $25 \times 40 \times 60$ mm with 4 mm total chamber thickness. It was fabricated with Dragon-skin-30, increasing rigidity for supporting the thumb. All casting molds and the robotic palm are fabricated by a commercially

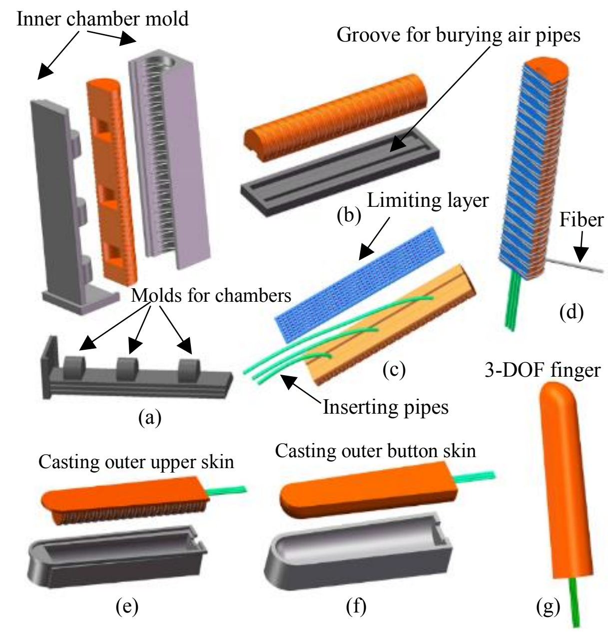

Figure.6. Fabrication of the fully-actuated soft robotic finger. (a) Molding the inner mold (b) Sealing inner mold. (c) Inserting pipes. Casting limiting layer. (d) Winding reinforced fiber. (e) Casting upper skin o. (f) Casting the bottom layer skin. (g) 3-DOFs soft finger.

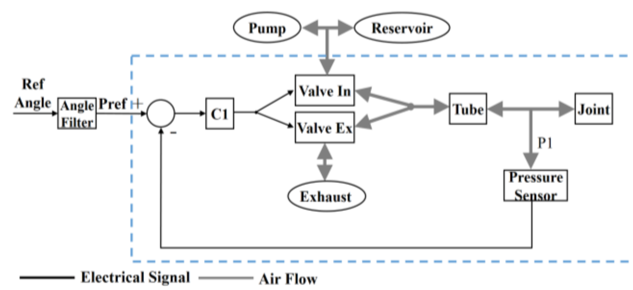

Figure 7. BCL-13 controller structure for a single joint. The dashed area presents the feedback control loop.

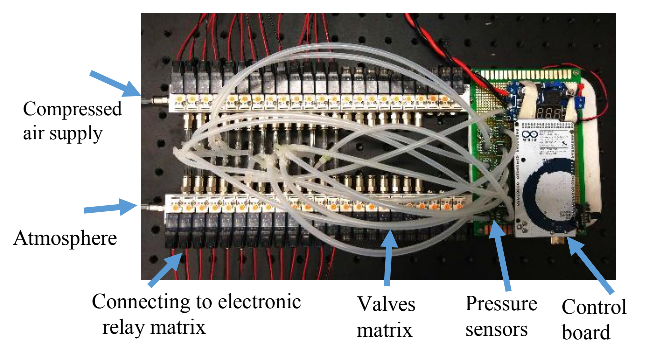

Figure 8. Dedicated pneumatic actuation system for BCL-13.

available delta 3D printer, with a material cost within US$10.

B. Actuation and control of BCL-13

The 13-DOF dexterity requires corresponding degrees of actuation and control. For each individual joint, a pressure-based controller (PBC) was formulated to regulate the input pressure and output motion, as introduced in our previous works [29, 30]. The control diagram for one joint is presented

This article has been accepted for publication in a future issue of this journal, but has not been fully edited. Content may change prior to final publication. Citation information: DOI 10.1109/LRA.2018.2851360, IEEE Robotics and Automation Letters

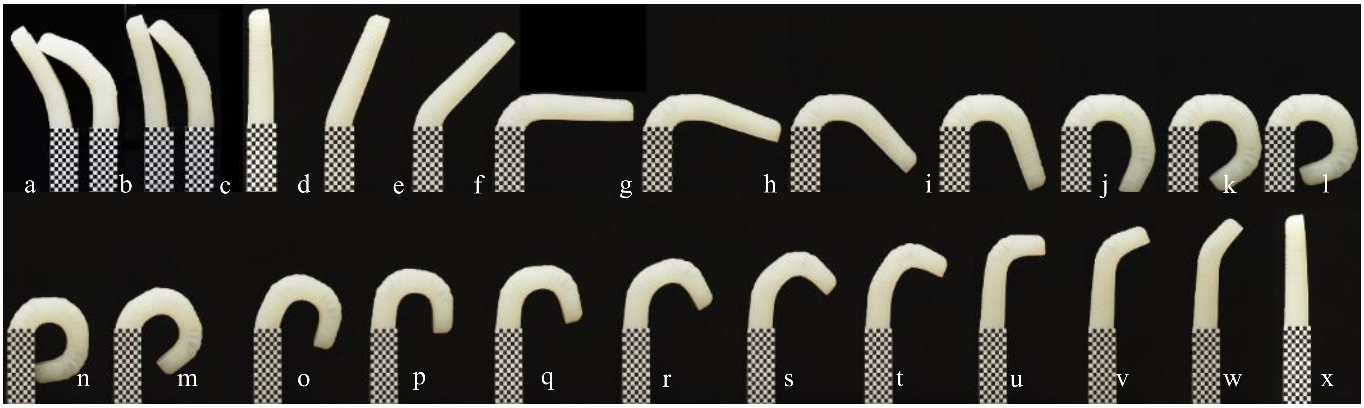

Figure 10.Finger workspace test. Figure (a,b) present the passive workspace of finger. Figure (c-l) present the finger flexion with the bending sequence MCP, PIP and DIP in order. Figure (n-x) present the extension with the opening sequence MCP, PIP and DIP in order.

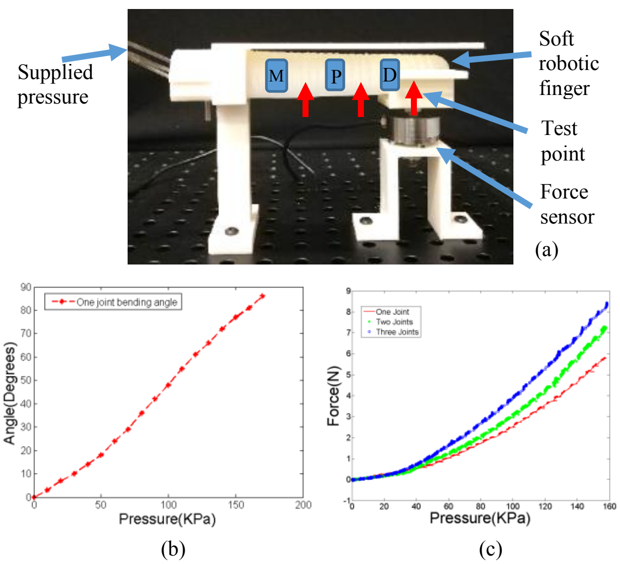

Figure 9. The soft robotic finger evaluation. (a) Finger force test platform. The finger with three joints DIP, PIP and MCP are illustrated by D, P and M respectively. (b) Finger bending angle test result. (b) Finger exertion force test result.

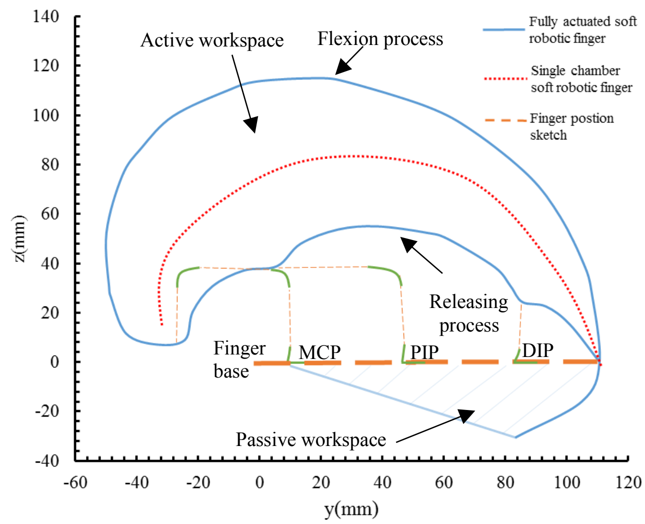

Figure 11.The measured workspace of proposed soft robotic finger and the counterpart trajectory of a predefined motion SPA. Existing 1-DOF soft fingers could only reach the dotted line, while the proposed 3-DOF SPA could reach the crescent planar similar with the human hand.

in Figure 7, composed of the angle filter, pressure controller (C1), two solenoid valves used to control the input\exhaust air, and a pressure sensor used to monitor the joint pressure. The angle filter can convert the anticipated bending angle of joint to a desired pressure value. The controller regulates the joint air pressure P1 to track the desired anticipated pressure (Pref). A control system with 13 pairs solenoid valves matrix (OST-10mm-11-12-L [32]: high speed two port valves with 50Hz maximum operating frequency) and 13 pressure sensors (Honeywell HSD-DANN060PGSA3), as shown in Figure 8, is built to control the motion for the BCL-13 hand. The BCL-13 hand weights 0.42 kg and the overall weight with actuation components is 1.27 kg.

IV. Experimental Validation

In this section, we present dedicated experiments to validate the effectiveness of the proposed BCL-13. The force and bending motion performances of each finger were tested. The intended workspace of the 3-DOF soft robotic finger is presented and discussed in details. Finally, the three intended modes of in-hand manipulations were validated.

A. Experiment Setup

A dedicated experimental platform is developed to test the exertion force and bending motion of soft fingers. The supplied air pressure was regulated by a pressure regulator valve (SMC ITV2030). Each joint was connected with a pressure sensor (Honeywell HSD-DANN060PGSA3). Single joint bending performance of the MCP joint was tested by varying the input pressure. To measure positions, footages of the finger motions were captured using a fix-mounted camera to the experiment platform. The captured images were then post-processed using object tracing to measure the bending angle and fingertip positions.

For force measurements, a proprietary platform developed in our previous work [19] was used as shown in Figure 9(a).

B. Finger Effectiveness Test

The motion and force capabilities of a single 3-DOF SPA finger were validated first. The results are shown in Figure 9b, showing a linear relationship between input pressure and bending angle with the maximum bending angle 86 degrees under 170 kPa. Compared to a typical human finger, the maximum bending angle of proposed robotic finger is very

This article has been accepted for publication in a future issue of this journal, but has not been fully edited. Content may change prior to final publication. Citation information: DOI 10.1109/LRA.2018.2851360, IEEE Robotics and Automation Letters

close to the human MCP (90 degrees) and DIP (90 degrees) joints, and smaller than the PIP (110 degrees) joints [1].

Force exertion capability tests were conducted on the test platform shown in Figure 9a [20, 28]. We tested the effective finger force under the end of each finger phalange as the red arrows shown. The test result is presented in Figure 9c. The maximum forces for the test points from the proximal to the distal phalanges were 5.7 N, 7.1N, and 8.5 N under 160 kPa input pressure, respectively. This trend is possibly caused by the inherent compliance of the SPA finger.

C. Finger Workspace Test

The proposed 3-DOF soft robotic finger could reach a large planar area comparable to the human finger. In addition, the soft-material passive compliance contributes to a further passive reachable area in addition to the active workspace. To validate this, a workspace test was conducted using camera-recorded actuator positions when sequentially pressurizing the chambers, with results as shown in Figure 10. The passive reachable area (Figure 10a-b) was achieved by actuating an opposing identical finger (right) to push a passive finger (left). In Figure 10c-l, the active flexion sequence is presented, with the flexion of MCP, PIP, and DIP sequentially. After the finger fully curved, each joint was released in reversing order, as depicted in Figure 10n-x. Tracing all finger-tip states of each figure, the maximum reachable area of the soft finger is obtained as depicted by the blue solid line in Figure 11. Compared to the crescent-shaped human finger workspace [26], the proposed soft finger workspace has a strikingly high similarity. The passive area extends from the natural equilibrium position, further expanding the range of motion in certain scenarios. Compare with single-chamber conventional soft actuators with single-trajectory motion range (red dotted line in Figure 11), the 3-DOF finger can reach substantially larger area, therefore enabling various grasping and in-hand manipulation features.

D. Hand Dexterity and Reliability Validation

To benchmark the outstanding dexterity of the soft robotic hand enabled by the 3-DOF fingers, a Kapandji test of hand dexterity was performed [31]. As presented in Figure 12a, the 13-DOF anthropomorphic hand can realize 8 of 10 Kapandji score test shown in Figure 12b, including Kapandji score III, IV, VI, VII, VIII, IX, and X as shown in Figure 12c-h. With the dedicated palm DOF, the thumb can touch all areas of the little finger and the distal volar crease of the hand. This test highlights the outstanding dexterity of the proposed 13-DOF soft robotic hand.

The proposed BCL-13 hand also shows excellent capabilities in object grasping by easily performing common grasping taxonomies on daily objects, as shown in Figure 13. Typical shapes of objects as cylinder, sphere, and disc can be grasped reliably with dedicated grasping taxonomies. With passive compliance, fruits and vegetables can be firmly grasped without risk of damage. An object-pull-out test, as shown in Figure 14, was conducted to demonstrate the grasping reliability of BCL-13. A 3D-printed sphere with diameter 90 mm and weight 110 g was used as the pulling out object forming a similar setup to our previous work [19].

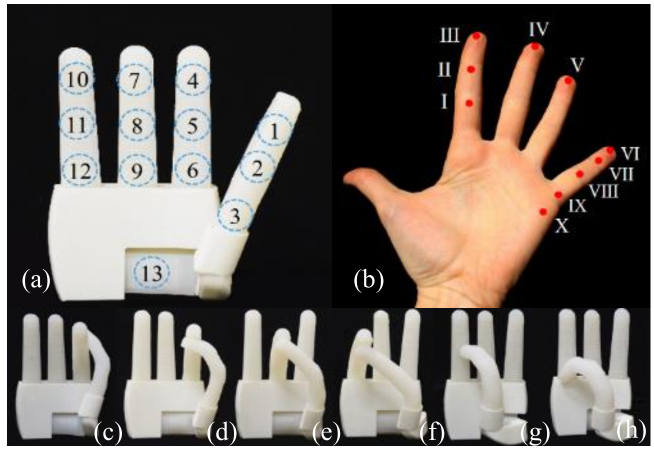

Figure 12. BCL-13 could achieve 8 out of 10 Kapandji scores. (a) BCL-13 with 13 joints. (b) 10 scores of Kapandji test. (c) Score II, touching DIP joint of index finger. (d) Score III, touching index finger-tip. (e) Score IV, touching middle finger-tip. (f-h) Scores VI-X. The thumb can touch all little finger and distal volar of hand.

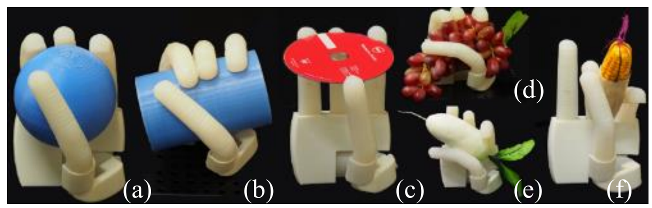

Figure 13. Typical shape objects grasping presentation. (a) Spherical object. (b) Cylindrical object. (c) Disc. (d) Grasp. (e) Radish. (f) Corn.

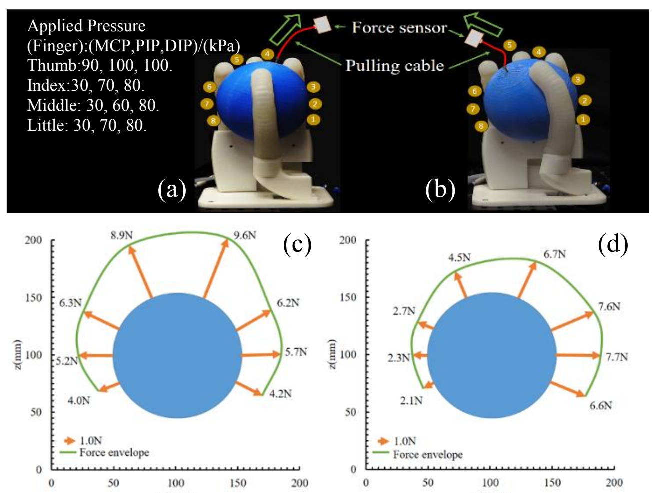

Figure 14. Object in-grasp pull away test. (a) Testing setup of 90 degree position (b) Testing setup of 60 degree position. (c) Testing result of 90 degree position. (d) Testing result of 60 degree position.

Forces required to pull the spherical object out from the BCL-13 hand in different directions in the vertical plane were compared with two different thumb positions, 90 degrees and 60 degrees as illustrated in Figure 14.a-b. The results were illustrated in Figure 14c-d, where the maximum pulling-out force could reach 9.6 N, and the force profile varied with the pulling directions. In addition, the thumb position also placed a significant impact on the resulting force profile, where turning the thumb 30 degrees to the right resulted in the pulling out force shifting considerably towards the same direction, as shown in Fig 14d. This demonstrates that hand

This article has been accepted for publication in a future issue of this journal, but has not been fully edited. Content may change prior to final publication. Citation information: DOI 10.1109/LRA.2018.2851360, IEEE Robotics and Automation Letters

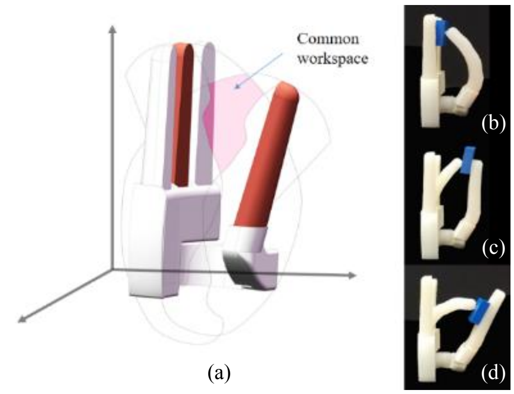

Figure 15. In-hand object translation test 1. (a) The common workspace between thumb and middle finger. (b-d) The moving process of the cubic.

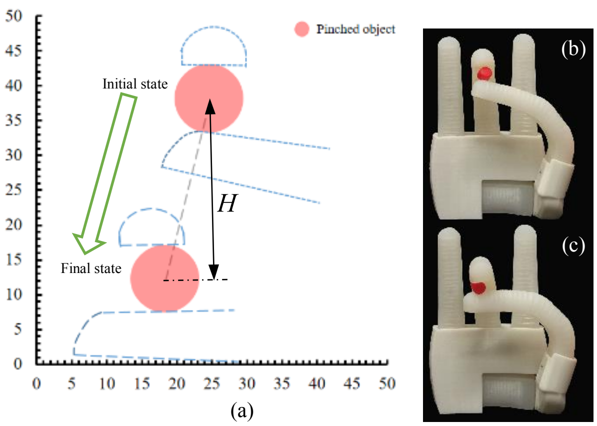

Figure 16. In-hand translation test 2. (a) Illustration of a red cylinder move down by thumb and middle finger. (b) The moving process of the cylinder.

dexterity plays a significant role both to grasping patterns and to grasping stability.

E. In-hand Manipulation Validation

In this subsection, the three modes of intended in-hand manipulations are experimentally validated: in-hand object translation, rotation, and reorientation.

Mode 1. Two translation tests were conducted. The first test was with parallel opposing fingers, as shown in Figure 14. With the thumb directly opposing the middle finger, they formed a common active workspace as the pink area shown in Figure 15a. The area was approximately 507 mm2. A blue test cube of 15x30x30 mm3 was pinched between the thumb and the middle finger. By coordinately actuating the two fingers as shown in Figure 15b-d, the hand can move the cube in y direction around 80 mm, which is 80% of the active length of the finger, and z direction at 20 mm, which is 20% active length of the finger.

Another in-hand translation test was with orthogonal opposing fingers, as shown in Figure 16b-c. A small red rubber cylinder was pinched by thumb and middle finger in an orthogonal setup. Actuating the two fingers moves the red cylinder vertically at a distance range of 22 mm, which is 22% of the active length of the finger.

Mode 2. The rotation test is presented in Figure 17b-d. A printed cylinder of 20 mm in radius and 25 mm in height was

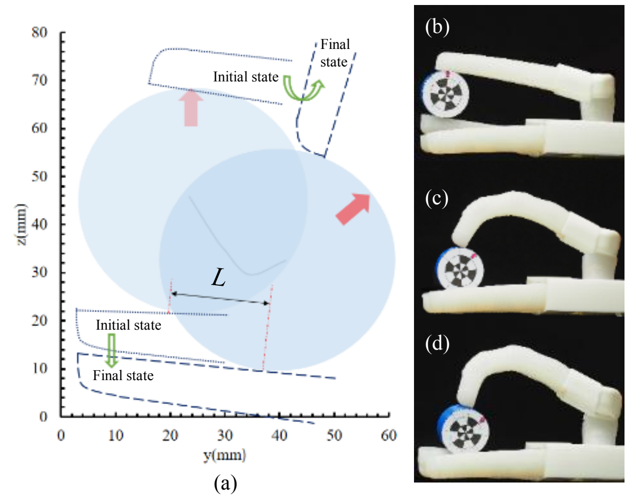

Figure 17. In-hand object rotation test. (a) The illustration of a cylinder rotated by thumb nad middle finger. (b-d) The rotation process of the cylinder.

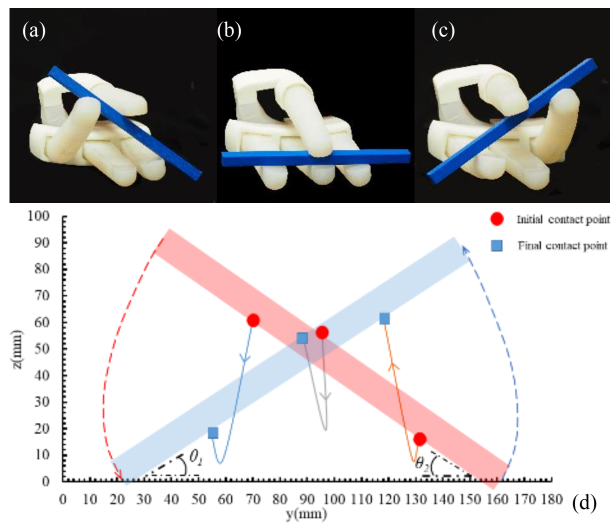

Figure 18. In-hand object reorientation test. (a-c) The reorientation process of a rod. (d) The illustration of the rod reorientation by thumb, index finger and little finger.

used for test, which covered with a mosaic marker used to facilitate image tracking. A red arrow on the cylinder marked the starting position. The cylinder was held between the thumb and the middle finger. By actuating the DIP and MCP joints of the thumb, the cylinder could be rotated in-hand as illustrated in Figure 17a, reaching a maximum rotation angle of 26 degrees and a maximum distance of 18 mm, or 18% of the active finger length.

Mode 3. As illustrated in Figure 18a-c, a blue test rod at 10x10x150 mm was held using three fingers: the thumb, index and little fingers. The thumb touched the center-of-gravity point of the rod, while the other two finger were actuated sequentially to rotate the rod while maintaining its fulcrum at the thumb, as shown in Figure 17. The rod can be manipulated in hand and the reorientation range is recorded in Figure 18d, with the measured range of rotation of 66 degrees (θ_1=32 degrees, θ_2=34 degrees).

The experimental results have demonstrated the superior dexterity of the proposed BCL-13 over the state-of-the-art soft robotic hands, enabled by the novel 3-DOF soft finger and the actuated palm, in both grasping and in-hand manipulation tasks.

V. Conclusions and Future Work

In this paper, a novel 3-DOF soft robotic actuator is presented. Using the novel actuator as fingers, a 13-DOF fully-actuated soft anthropomorphic robotic hand was proposed with high dexterity. The 3-DOF bio-inspired SPA finger had three human-like joints which can be actuated independently, thus it could reach a human-finger-like workspace rather than a predefined curve trajectory as in existing single-chamber SPAs. This human-like workspace enabled the proposed robotic finger with dexterous grasping capability in robotic hand applications, especially for in-hand manipulation. A four-fingered anthropomorphic hand, with a total of 13 DOFs, was presented to achieve 3 modes of in-hand manipulation, including in-hand object translation, in-hand object rotation, and in-hand object reorientation. The experiment results demonstrated that the proposed robotic hand could successfully achieve the anticipated in-hand manipulation functionalities. Fabrication procedure and experiment procedures were presented in detail, to validate the effectiveness of the proposed soft robotic finger and the anthropomorphic hand. The presented approach provided a promising candidate for dexterous anthropomorphic robotic hand design, which could potentially work as prosthetics or robotic hands interacting with humans.

Future works include: characterizing the multi-DOFs SPA behavior for further design refinements; modeling of the soft finger joint to realize accurate bending control and providing design instruction for the designer; control investigations with positional feedback, to enable the soft robotic finger for real-time interaction feedback. With demonstrated superior dexterity and preliminary in-hand manipulation capabilities, this work paves the way towards a soft robotic approach for dexterous robotic hand performance in functionality, morphology and anthropomorphism.

References

[1] Napier J R, Tuttle R H. *Hands*. Princeton University Press, 1993.

[2] Bicchi A, Kumar V. Robotic grasping and contact: a review. IEEE International Conference on Robotics and Automation, 2000. Proceedings. ICRA. IEEE, 2002:348--353.

[3] Okamura A M, Smaby N, Cutkosky M R. An Overview of Dexterous Manipulation. IEEE International Conference on Robotics and Automation, ICRA 2000, April 24-28, 2000, San Francisco, Ca, USA. IEEE Xplore, 2000:255-262.

[4] Bullock I M, Ma R R, Dollar A M. A Hand-Centric Classification of Human and Robot Dexterous Manipulation. IEEE Computer Society Press, 2013.

[5] Salisbury J K, Craig J J. Articulated hands: Force control and kinematic issues. *The International Journal of Robotics Research*, 1982, 1(1): 4-17.

[6] Butterfass, J., Grebenstein, M., Liu, H., & Hirzinger, G . DLR-Hand II: next generation of a dextrous robot hand. IEEE International Conference on Robotics and Automation, 2001. Proceedings. IEEE, 2001:109-114 vol.1.

[7] Kawasaki H, Komatsu T, Uchiyama K. Dexterous anthropomorphic robot hand with distributed tactile sensor: Gifu hand II. *IEEE/ASME Transactions on Mechatronics*, 2002, 7(3): 296-303.

[8] Rojas N, Ma R R, Dollar A M. The GR2 Gripper: An Underactuated Hand for Open-Loop In-Hand Planar Manipulation. *IEEE Transactions on Robotics*, 2016, 32(3):763-770.

[9] Bicchi A. Dexterous Grippers: Putting Nonholonomy to Work for Fine Manipulation. *International Journal of Robotics Research*, 2002, 21:427-442.

[10] Shadowrobot. 2018. Shadowrobot. [ONLINE] Available at: https://www.shadowrobot.com/. [Accessed 21 February 2018].

[11] Xu Z, Todorov E. Design of a highly biomimetic anthropomorphic robotic hand towards artificial limb regeneration IEEE International Conference on Robotics and Automation. IEEE, 2016:3485-3492.

[12] Odhner, L. U., Jentoft, L. P., Claffee, M. R., Corson, N., Tenzer, Y., Ma, R. R., & Dollar, A. M. A compliant, underactuated hand for robust manipulation. *International Journal of Robotics Research*, 2014, 33(5):736-752.

[13] Ma R, Dollar A. Yale OpenHand Project: Optimizing Open-Source Hand Designs for Ease of Fabrication and Adoption. *IEEE Robotics & Automation Magazine*, 2017, 24(1):32-40.

[14] Howe R D, Cutkosky M R. *Touch sensing for robotic manipulation and recognition*. The robotics review 2. MIT Press, 1992.

[15] Shen H. Meet the soft, cuddly robots of the future. *Nature*, 2016, 530(7588):24.

[16] Rus, D., & Tolley, M. T. (2015). Design, fabrication and control of soft robots[J]. *Nature*, 521(7553), 467-75.

[17] Wang Z, Hirai S. A Prestressed Soft Gripper: Design, Modeling, Fabrication, and Tests for Food Handling. *IEEE Robotics & Automation Letters,* 2017, 2(4):1909-1916.

[18] Gaiser, I., Schulz, S., Kargov, A., & Klosek, H. (2008). A new anthropomorphic robotic hand. Humanoids 2008, Ieee-Ras International Conference on Humanoid Robots (pp.418-422). IEEE.

[19] Zhou J, Chen S, Wang Z. A Soft Robotic Gripper with Enhanced Object Adaptation and Grasping Reliability. *IEEE Robotics & Automation Letters*, 2017, 2 (4):2287-2293.

[20] Ilievski, F., Mazzeo, A. D., Shepherd, R. F., Chen, X., & Whitesides, G. M. (2011). Soft robotics for chemists. *Angewandte Chemie International Edition*, 50(8), 1890-1895.

[21] Deimel R, Brock O. A compliant hand based on a novel pneumatic actuator. Robotics and Automation (ICRA), 2013 IEEE International Conference on. IEEE, 2013: 2047-2053.

[22] Deimel, R., & Brock, O. (2015). A novel type of compliant and underactuated robotic hand for dexterous grasping. *International Journal of Robotics Research*, 35(1), 161-185.

[23] Zhao, H., O'Brien, K., Li, S., & Shepherd, R. F. Optoelectronically innervated soft prosthetic hand via stretchable optical waveguides. *Science Robotics*, 1(1), eaai7529. 2016.

[24] Marchese, A. D., Katzschmann, R. K., & Rus, D.. A recipe for soft fluidic elastomer robots. *Soft Robot*, 2015, 2(1), 7-25.

[25] Polygerinos, P., Wang, Z., Overvelde, J. T., Galloway, K. C., Wood, R. J., Bertoldi, K., & Walsh, C. J. Modeling of soft fiber-reinforced bending actuators. *IEEE Transactions on Robotics*, 2015, 31(3), 778-789.

[26] Peer A, Einenkel S, Buss M. Multi-fingered telemanipulation - mapping of a human hand to a three finger gripper. The IEEE International Symposium on Robot and Human Interactive Communication, 2008. Ro-Man. IEEE, 2008:465-470.

[27] Wang, Z., Polygerinos, P., Overvelde, J., Galloway, K., Bertoldi, K., & Walsh, C. Interaction forces of soft fiber reinforced bending actuators. *IEEE/ASME Transactions on Mechatronics*, 2017, 22(2), 71-727.

[28] Chen, X., Peng, J., Zhou, J., Chen, Y., Wang, M. Y., & Wang, Z. A robotic manipulator design with novel soft actuators. In Robotics and Automation (ICRA), 2017 IEEE International Conference on (pp. 1878-1884). May 2017.

[29] Polygerinos, P., Wang, Z., Galloway, K. C., Wood, R. J., & Walsh, C. J. Soft robotic glove for combined assistance and at-home rehabilitation. *Robotics and Autonomous Systems*, 2015, 73, 135-143.

[30] Yi, J., Chen, X., Song, C., & Wang, Z. Fiber-Reinforced Origamic Robotic Actuator. *Soft robotics*, 2018, 5(1), 81-92.

[31] Kapandji A. Clinical test of apposition and counter-apposition of the thumb. *Ann Chir Main*, 1985, 5(1):67-73.

[32] OST Solenoid Valves, www.//ours-top.com/. [Accessed 19 May 2018].

[33] Sturman D J. *Whole-hand input*. Massachusetts Institute of Technology, 1992.